ICAS 2021 SHANG HAI
International Council of the Aeronautical Sciences
32nd Congress of the International Council of the Aeronautical Sciences
September 6-10, 2021
Pudong Shangri-La, Shanghai, China

EXPERIMENTAL STUDY ON ATTENUATION PERFORMANCE OF SHOCK-ABSORBING INSERT

Hyun-Su Park[1], Dae-Hyun Hwang[1], Jinkyu Yang[2] & Jae-Hung Han[1]

[1]Department of Aerospace Engineering, KAIST

Daejeon 34141, Republic of Korea

[2]Department of Aeronautics and Astronautics, University of Washington

Seattle, WA 98195, United States

Abstract

Pyrotechnic separation devices have been widely used in aerospace industries in order to separate structural parts with high reliability. Although they have advantages of high reliability and cost-effectiveness, the devices generate an intensive dynamic response called pyroshock, which can lead to fatal damage to mounted small electronic equipment. In this study, a novel design of a sandwich panel insert is proposed to achieve enhanced shock attenuation. In order to evaluate the attenuation performance, shock propagation experiments and numerical analysis were carried out. The results show that the shock-absorbing insert can effectively reduce propagating shock for the joint structure.

Keywords: Pyroshock, Honeycomb sandwich panel, Sandwich panel insert, Shock absorber

1. Introduction

Pyroshock is generated by pyrotechnic-based separation devices, which are often used for stage or payload separation of space vehicles and in many other aerospace applications such as pilot ejection. With a high frequency component exceeding 2 kHz, pyroshock has a magnitude that may reach 100,000 g. These characteristics of pyroshock rarely cause structural deformation, but the high frequency component is known to cause possible failures of small electronic equipment mounted on the structures of vehicles [1-2]. To prevent this problem, it is important to predict the propagation path and the attenuation level of the shock. In the case of a honeycomb sandwich panel, which is widely used in the aerospace industry, inserts are frequently used to connect structures and the shock propagates through this insert system. In general, a shock wave propagates in an elastic wave form, and thus the magnitude of the shock is attenuated at the joints [3-4]. From this point of view, inserts can be designed in such a way that the propagated shock is effectively attenuated.

In this paper, a shock-absorbing insert is developed and a shock propagation experiment is conducted to identify the attenuation performance of this new type of insert. Elastomeric materials, such as rubber and polyurethane, are used for the shock absorption in this insert. The honeycomb panel and the plate are joined with bolt connection of the inserts and the pyroshock simulator generates shock on the plate. The shock wave propagates through the insert system to the honeycomb sandwich panel. By comparing the shock magnitude of the plate and the honeycomb panel, the shock attenuation performance of the insert system can be identified. To measure shock quantitatively, the shock response spectrum (SRS) was used.

Furthermore, it is important to establish a numerical analysis methodology for the honeycomb sandwich panel because it is not easy to perform repeated experiments. When the insert is installed on the honeycomb sandwich panel, it is difficult to remove and reinstall. In this study, a methodology for the analysis of the shock-absorbing insert is proposed and the analysis results are compared with the experimental results to verify the accuracy of the numerical analysis.

2. Design of Sandwich Panel Insert

2.1 Conventional Insert

Honeycomb sandwich panels are widely used in the aerospace industry due to their high stiffness-weight ratio. To mount equipment or connect joints, sandwich panel inserts are used. The general shape of the insert is a cylindrical structure with two flanges at the bottom and top. Based on the Insert Design Handbook [5] published by the European Space Agency (ESA), we made a conventional insert for an M5 bolt connection. The outer diameter of the insert was 17 mm and the height was 12 mm. Stainless steel, 304 SS, was employed for the material of the insert. The basic method to install inserts on the honeycomb sandwich panel is to inject epoxy resin into holes in the upper flange.

Figure 1 – Conventional insert

2.2 Shock-Absorbing Insert

A conceptual design of the shock-absorbing insert is shown in Figure 2. There are four parts to be assembled: housing, insert core, elastomer washer, and cap. The housing has a space for the insert core with elastomer washers and a thread to connect with the cap. It was made with an outer diameter of 22 mm and a height of 16 mm. Both the diameter and the depth of the inner space were 14 mm.

The insert core has bolt thread for M5 bolt connection and it was positioned in the housing with elastomer washers. Two elastomer washers were positioned above and below the insert core. The outer diameter was 13 mm and the height was 14 mm. Ethylene Propylene Diene Monomer (EPDM) and Polyurethane (PU), widely used as shock-absorbing materials in the aerospace field [6], were employed for the elastomer in this study. The height, outer diameter, and inner diameter of the elastomer washer were 3 mm, 14 mm, and 9 mm, respectively.

The cap has a thread in the radial direction to connect with the housing. Torque was applied to the gaps in the cap by using a ratchet wrench. The cap has an outer diameter of 14 mm, an inner diameter of 10 mm, and a height of 4 mm. The assembly procedure is as follows: (1) The elastomer washers are put on the insert core; (2) The insert core with washers is inserted into the housing; (3) Torque is applied to the cap using a ratchet wrench. The main role of the cap is to limit the vertical movement of the insert core. The material for the elastomer washers can be replaced without difficulty according to the required performance or the operating environment by opening the cap.

The proposed structure is easy to assemble and the installation procedure is the same as that for the conventional insert. All parts except the washers are made of 304 SS. Due to the impedance breakdown between 304 SS and the elastomer in the inner structure, the shock is effectively attenuated.

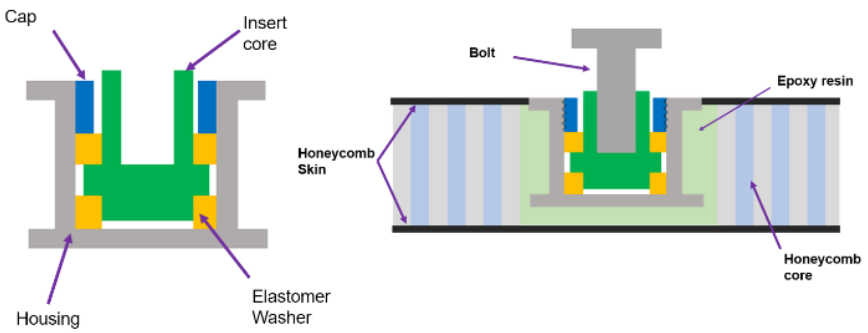

Figure 2 – Conceptual design of the shock-absorbing insert

Figure 3 – Shock-absorbing insert

3. Shock Propagation Experiment

3.1 Experimental Setup

A simple plate (600 mm x 400 mm x 5 mm) made out of aluminum-6061 and two aluminum honeycomb sandwich panels (600 mm x 400 mm x 20 mm) with 1 mm skin thickness were prepared to conduct the shock propagation experiment. The panels have eight holes at 50 mm intervals to install the inserts, as shown in Figure 4. In order to investigate the attenuation performance of different types of elastomer materials, EPDM and PU washers were prepared. PU is relatively stiffer than EPDM. The elastomer was easily replaced by opening the cap of the shock-absorbing insert. The honeycomb sandwich panel and the plate were connected by a bolted joint. This model was suspended using four cables, as shown in Figure 5, and a free boundary condition was achieved.

For non-contact velocity measurement, an LDV (Laser Doppler Vibrometer) was used. There were two measurement points, as shown in Figure 5, and they were 100 mm apart from the joint region. Velocity measurements were performed at a sampling frequency of 1 MHz for 20 ms. After the LDV measurements, a band-pass filter for 100 to 100,000 Hz was applied, and the acceleration in the time domain was obtained by differentiating the velocity. In order to quantify the measured shock, the Shock Response Spectrum (SRS) was obtained. The SRS indicates the maximum acceleration value obtained by applying time-domain acceleration on the Single Degree of Freedom (SDOF) system corresponding to each natural frequency. In general, the damping ratio of an SDOF system is 0.05 (the Q factor is 10) [7]. The SRS is the most commonly used method to analyze the shock because it is easy to identify the possibility of damage due to shock in each frequency band. By comparing the SRS of two points, the shock attenuation of the inserts could be identified.

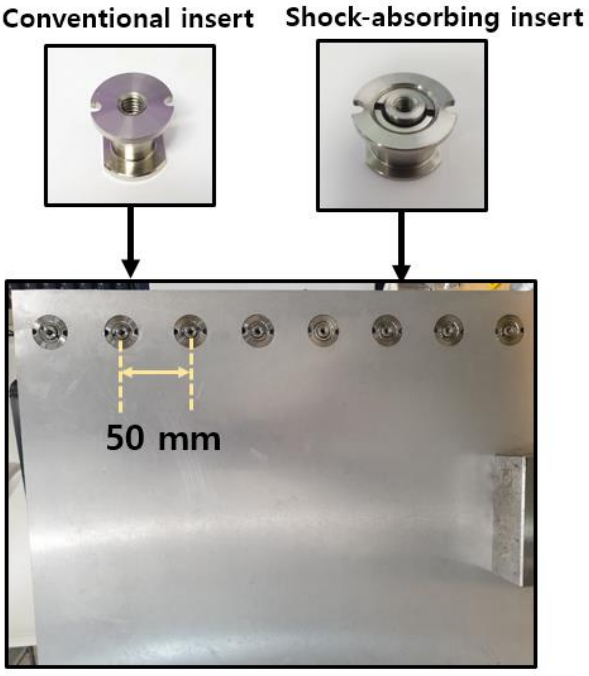

Figure 4 – Inserts installed on the panel

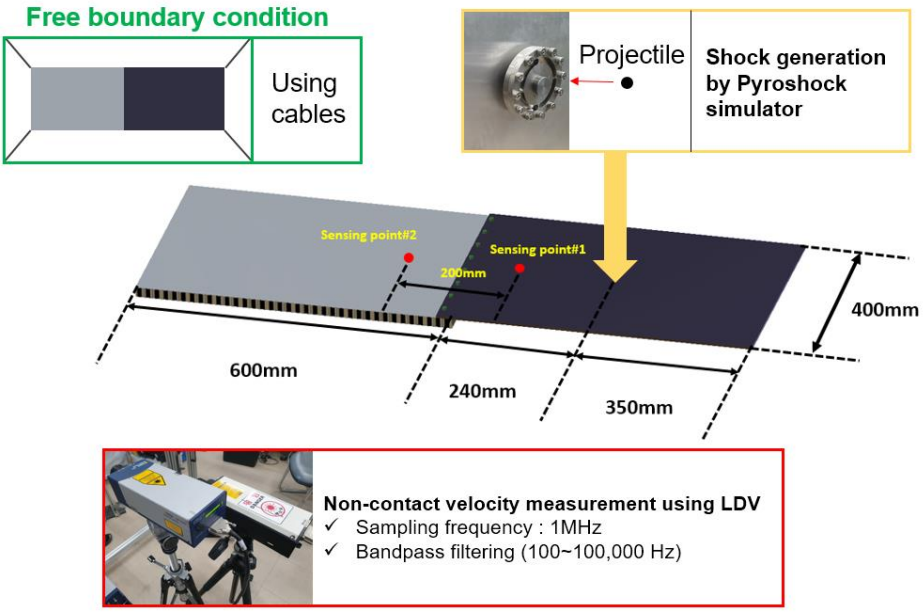

Figure 5 – Experimental setup [8-9]

3.2 Results

The SRS results of the experiment are presented in Figure 6 [9]. Furthermore, the SRS results according to the sensing points shown in Figure 7 and 8 compare three selected cases: the conventional insert and shock-absorbing inserts with EPDM and PU. Similar results were observed for all the sensing point #1 results, indicating that the generated shock has excellent repeatability. Also, the knee frequency is about 7200 Hz, the slope of the growing region is 9.7 dB/octave on average, and the maximum acceleration is about 15,000 G. This means that the shock generated by the pyroshock simulator meets the pyroshock criteria [10]. From the sensing point #2 results, the shock-absorbing insert showed better attenuation performance than the conventional insert, and EPDM was better than PU for shock absorption due to its lower stiffness. To quantify the attenuation performance of the inserts, the SRS variance between sensing point #1 and sensing point #2 was calculated in dB unit and is shown in Figure 9. SRS variance of -15 dB means that the shock of sensing point #2 was attenuated by 83% compared to the SRS of sensing point #1. The shock response in the high frequency range (above 2kHz) was reduced by more than 83% for the shock-absorbing inserts with EPDM. This range of frequency is a risk factor to mounted small electronic equipment, and the applicability of the shock-absorbing insert was investigated for the shock attenuation during the propagation.

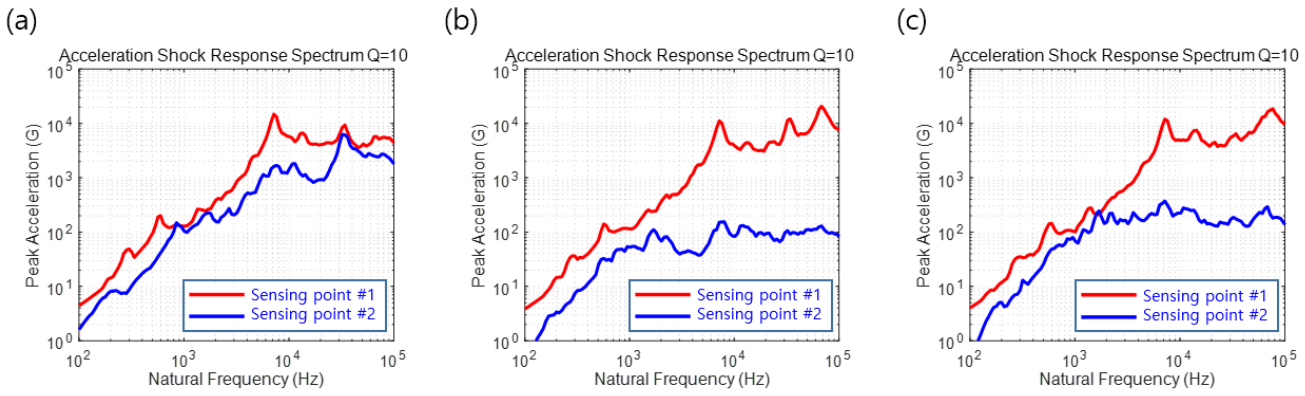

Figure 6 – Results of the experiment (a) conventional insert (b) shock-absorbing insert with EPDM (c) shock-absorbing insert with PU [9]

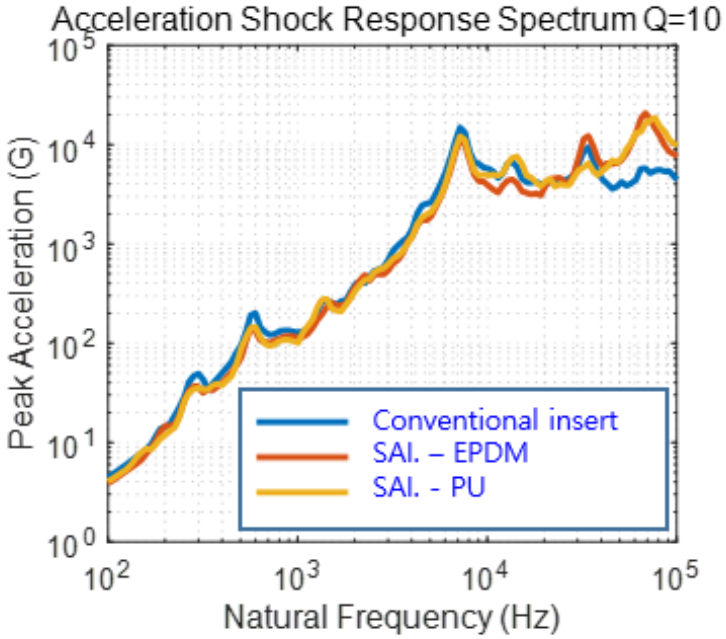

Figure 7 – Results for sensing point #1

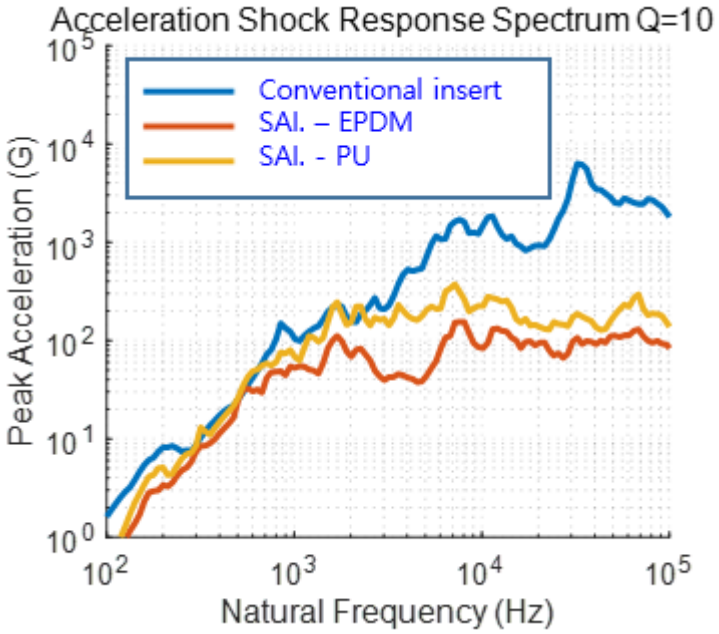

Figure 8 - Results for sensing point #2

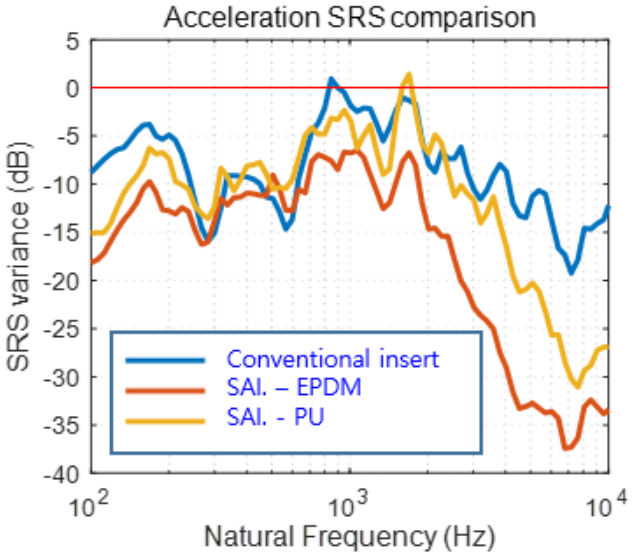

Figure 9 – Shock attenuation performance

4. Numerical Analysis

4.1 Methodology

4.1.1 Structure Modeling

The honeycomb sandwich panel consists of a honeycomb core and two thin skins. The core and skins are very thin, and to simulate this feature, a shell-like structure was used. Due to the advantage of cost-efficiency, the shell structure is widely used for thin models. In this study, a half model was made using a symmetry boundary condition. Four holes for inserts were also modeled, as shown in Figure 10. In this analysis, only the shock-absorbing insert with EPDM, which showed the best attenuation performance in the experiment, was simulated using ANSYS AUTODYN.

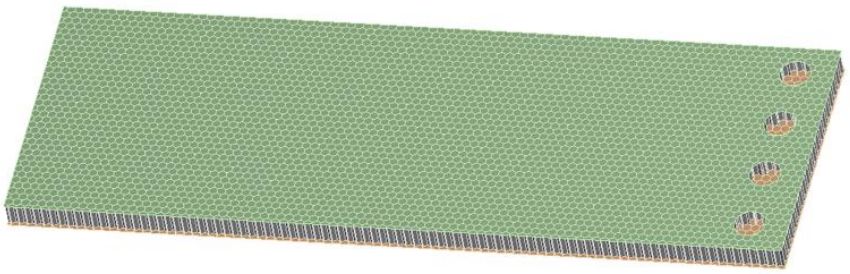

Figure 10 – Honeycomb sandwich panel for the numerical analysis

The epoxy resin, which is used for the bonding between the panel and inserts, was modeled with an effective potting radius. Due to the shape of the honeycomb core, a form of epoxy resin is irregular for each hole. However, this irregularity makes low quality elements, and it increases analysis time. The Insert Design Handbook suggests a concept of an effective potting radius, which assumes that the form of epoxy resin is cylindrical [5]. From the formula below, cylindrical epoxy resin with a radius of 17 mm was made (Figure 11).

$$r_{eff} = 1.002064\, r_i + 0.940375\, S_c - 0.7113 \quad (1)$$

$$r_{eff}: effective\ potting\ radius \quad r_i: insert\ radius \quad S_c: cell\ size$$

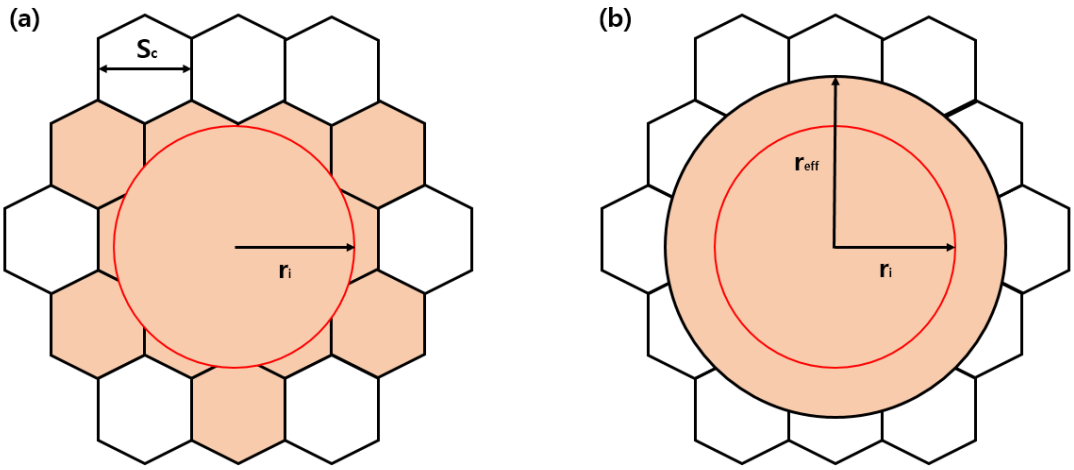

Figure 11 – Shape of epoxy resin (a) actuality (b) using effective potting radius

Parts of the shock-absorbing insert were modeled using a solid structure as shown in Figure 12. Bonded boundary conditions were applied to the thread region. Frictional boundary conditions were applied to the other contact regions and the coefficient of friction was 0.2. For the region where the shock is generated, an additional flat disk was modeled.

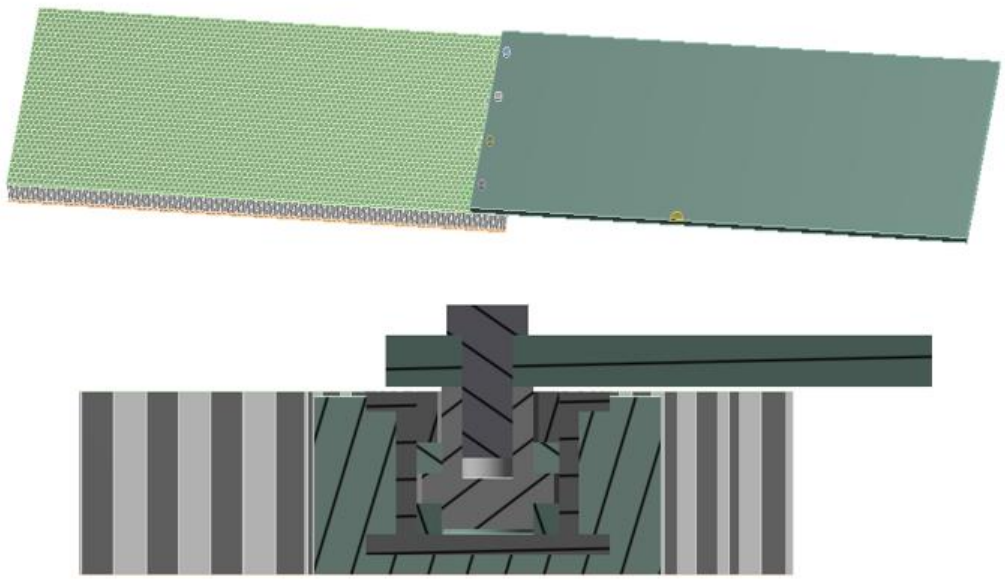

Figure 12 – Full model for the numerical analysis

4.1.2 Shock Generation

In the experiment, the shock was generated by launching a projectile with high velocity. However, this is difficult to precisely simulate. In this analysis, a velocity boundary condition was applied to the flat disk (Figure 13). The position of the disk is the same as the location of shock generation. From the previous experiment, the velocity of the location was obtained. The obtained data, velocity over initial 3 ms, was applied to the disk. This method was performed and verified by Lee *et al* [4].

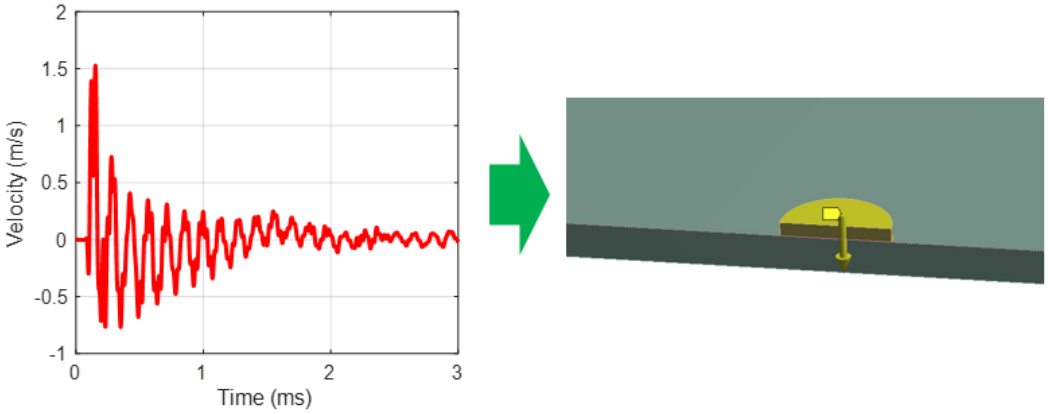

Figure 13 – Velocity boundary condition applied to the disk

4.1.3 Meshing

For accurate analysis, it is important to generate appropriate elements. If the shape of the element is extremely asymmetric or there are too many elements, the analysis time is considerably increased. Conversely, if the element size is too large and the number is insufficient, the accuracy of the analysis is very poor [11-12]. In particular, the size of the element in the analysis of the shock propagation is critical because it determines the analysis time interval and the detection frequency band. In this study, the size of the shell element was 2 mm, and that of the solid element was 1.5 mm.

A 4-node explicit thin structural shell element (SHELL 163) was applied to the honeycomb sandwich panel and an 8-node explicit structural solid element (SOLID164) was applied to the plate and the disk. For the other parts, a 10-node explicit tetrahedral structural solid element (SOLID168) was used (Figure 14).

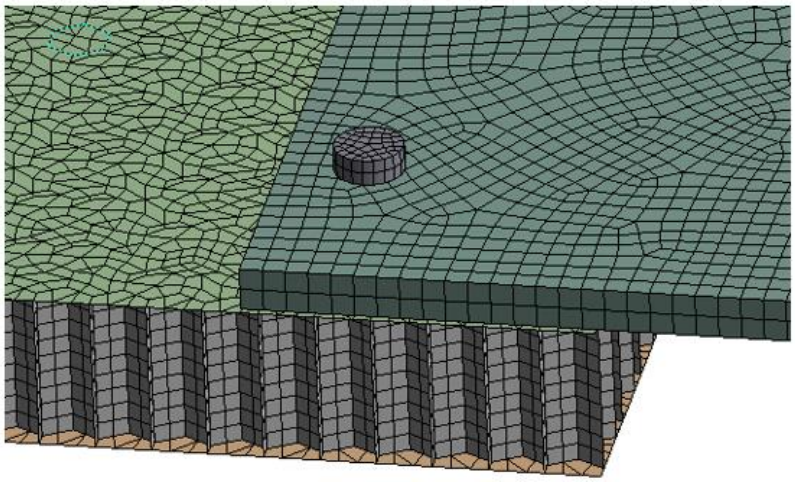

Figure 14 - Finite element model

4.2 Results

The analysis was performed for 10 ms and the time interval was 10^{-5} ms. As in the experimental study, there were two measurement points, which were located 100 mm apart from the joint region. The SRS results of the analysis are shown in Figure 15. The results show that the attenuation performance of the shock-absorbing insert with EPDM is outstanding in the high frequency band. A comparison of experimental and analytical SRS results is presented in Figure 16. Due to the insufficient analysis time, there was a slight difference in the low frequency band. On the other hand, the results in the high frequency band showed excellent accuracy. Also, from the comparison of the attenuation performance shown in Figure 17, the attenuation performance is similar in the experiment and the analysis. From both studies, the attenuation performance of the shock-absorbing

insert was investigated and the applicability of the insert was verified.

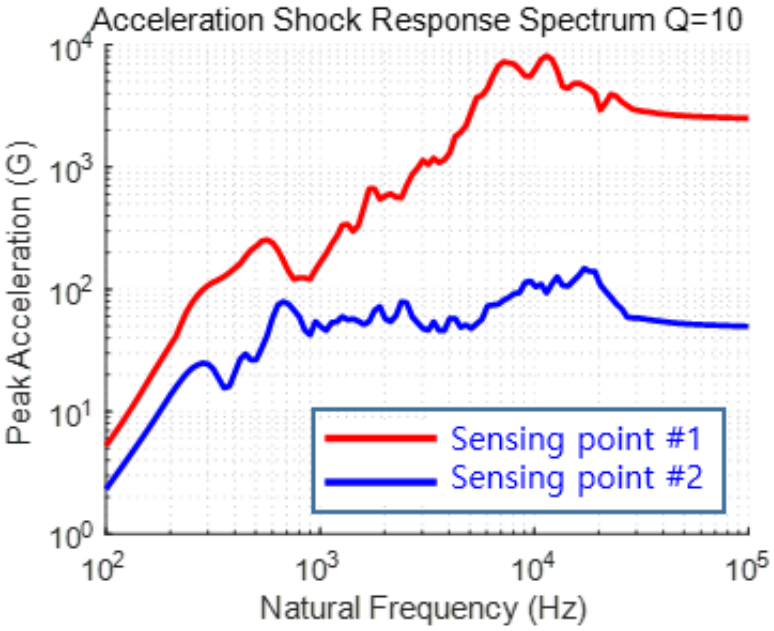

Figure 15 – Results of the numerical analysis

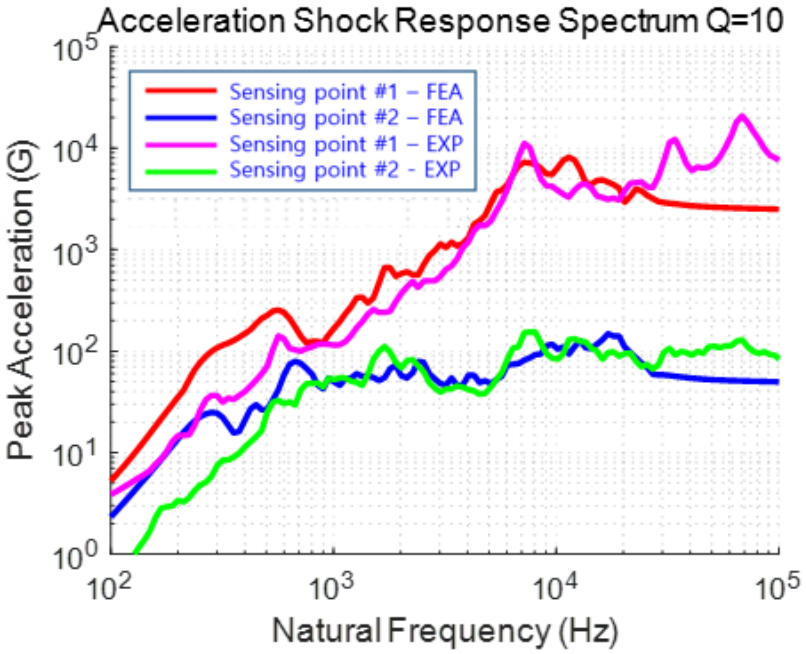

Figure 16 - Comparison of SRS results

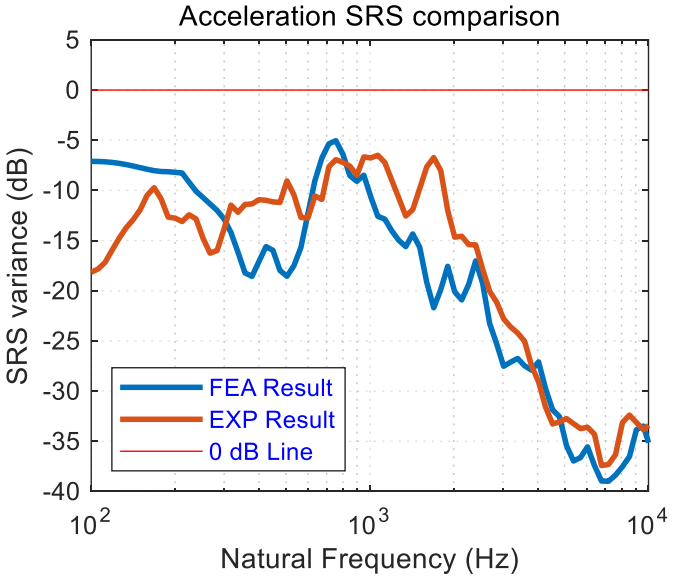

Figure 17 – Comparison of attenuation performance

5. Concluding Remarks

In this study, a novel design of a sandwich panel insert for shock attenuation was proposed, and its applicability to an aerospace structure was investigated. The shock-absorbing insert was developed to induce impedance breakdown in its inner structure. Elastomer washers played the key role as the shock attenuator due to their low stiffness. The shock attenuation performance of both inserts was also evaluated by conducting shock propagation experiments and a numerical analysis.

This study found that the shock-absorbing insert reduced the high-frequency shock during propagation through a honeycomb structure. In addition, a methodology for a numerical analysis was established and verified through a comparison of experimental and analytical results. The novel shock-absorbing insert has easy accessibility and a powerful shock-absorbing mechanism; it may be used to protect the small electronic equipment mounted on a honeycomb sandwich panel from severe shock.

6. Acknowledgments

This research was supported by the MSIT (Ministry of Science, ICT), Korea, under the High-Potential Individuals Global Training Program (2019-0-01598) supervised by the IITP (Institute for Information & Communications Technology Planning & Evaluation).

7. Contact Author Email Address

jaehunghan@kaist.ac.kr

8. Copyright Statement

References

[1] Pyroshock, MIL-STD-810G Method 517.1, Department of Defense, USA, 2008.

[2] European Cooperation for Space Standardization, *Mechanical shock design and verification handbook*, ECSS-E-HB-32-25A, , European Space Agency, Noordwijk, Netherlands , 2015.

[3] Moening CJ. Pyrotechnic shock flight failures, *Proceedings of Institute of environmental sciences pyrotechnic shock tutorial program*, 31st Annual Technical Meeting of the Institute of Environmental Sciences (IES), pp 4-5, 1985.

[4] Lee J, Hwang DH and Han JH. Study on pyroshock propagation through plates with joints and washers, *Aerospace Science and Technology*, Vol. 79, pp 441-458, 2018.

[5] European Cooperation for Space Standardization, *Insert Design Handbook*, ECSS-E-HB-32-22A, European Space Agency, Noordwijk, Netherlands, 2011.

[6] Jung BH, Kim YW, Lee JR and Kim DS. Visualization of pyroshock wave reduction by insulator using a laser shock based simulation method, *Measurement*, Vol. 137, pp 302-311, 2019

[7] Irvine T. *An introduction to the shock response spectrum*, Revision S, Vibrationdata, 2012.

[8] Hwang DH, Park HS and Han JH. Development of a miniature point source pyroshock simulator, *Journal of Sound and Vibration*, Vol. 481, Article No. 115438, 2020.

[9] Park HS, Hwang DH, Yang JK and Han JH. Development of shock-absorbing insert for honeycomb sandwich panel, *Aerospace Science and Technology*, Vol. 104, Article No. 105930, 2020.

[10] Pyroshock Test Criteria, NASA Technical Standard, NASA-STD-7003, 2011.

[11] Hwang DH, Lee J, Han JH, Lee Y and Kim D. Mathematical model for the separation behavior of low-shock separation bolts, *Journal of Spacecraft and Rockets*, Vol. 55, No. 5, pp 1208-1221, 2018.

[12] Hwang DH, Han JH, Lee J, Lee Y and Kim D. A mathematical model for the separation behavior of a split type low-shock separation bolt, *Acta Astronautica*, Vol. 164, pp 393-406, 2019.